Contract No.:

This manuscript has been authored by Savannah River Nuclear Solutions (SRNS), LLC under Contract No. DE-AC09-08SR22470 with the U.S. Department of Energy (DOE) Office of Environmental Management (EM).

Using a Coupled Dispersion Model to Estimate Depletion of a Tritium Oxide Plume by a Forest

Brian J. Viner[a]
Sydney Goodlove[a]

[a] Savannah River National Laboratory
203 Laurens St SW
Aiken, SC 29802

Corresponding Author: Brian J. Viner
Savannah River National Laboratory
Bldg. 773-A A-1009
Aiken, SC 29802
Brian.Viner@srnl.doe.gov

Abstract

Tritium processing facilities may release tritium oxide (HTO) to the atmosphere which poses potential health risks to exposed co-located workers and to offsite individuals. Most radiological consequence analyses determine HTO dose by applying Gaussian plume models to simulate the transport of HTO. Within these models, deposition velocity is used to assess the sum of all deposition processes acting on the plume. While this may account for vegetative and soil uptake or respiration processes, it may currently lack inclusion of the complex interactions within heterogeneous forested environments. In this complex morphology, dispersion patterns are significantly altered by changing flow regimes above and below the forest canopy and by the transfer of plume material across the canopy boundary. To determine the effects of a heterogeneous forest canopy on an airborne HTO plume, a Gaussian plume model coupled with an advection-diffusion plume model was applied to estimate transport in the free atmosphere above the forest and within the forest canopy and understory. During 2012, wind speed and wind direction measurements taken at 5 heights, ranging from 2-m to 28-m, on an instrumented meteorological tower located in a loblolly pine forest at the Department of Energy (DOE) Savannah River Site (SRS), near Aiken, SC. From these measurements, model predictions were made over a full spectrum of meteorological conditions. Deposition and resuspension velocities were calculated based on the model-predicted flux of plume material across the top of the forest canopy. Additionally, net deposition velocity of the plume material was calculated as the difference between the deposition and resuspension velocities. The 1st and 5th percentile net deposition velocities were estimated to be 0.7 cm s^{-1} and 1.2 cm s^{-1}, respectively.

1. Introduction

Releases of tritium to the atmosphere from the operation of nuclear reactors, reprocessing plants, and tritium processing facilities may result in potential health risks to facility workers, co-located workers, and the public. Most atmospheric releases of tritium consist primarily of its elemental (HT) or oxide (HTO) forms (Kessler, 1983). HT is a low-energy beta emitter with inhalation as the primary dose pathway. However, HTO exposure is of much greater concern due to its molecular similarity to water which is readily exchanged in plants and organic tissue (Ojovan and Lee, 2005), and then rapidly distributed throughout the body, leading to cell damage as it undergoes radioactive decay. Accordingly, HTO has a significantly larger Dose Conversion Factor (DCF) than HT, posing a much greater risk to human health (EPA, 1988).

To reduce potential radiological consequences from HT and HTO releases, Material at Risk (MAR) limits may be placed on tritium processing facility inventories and/or production levels. These administrative controls are typically determined by radiological consequence assessments using atmospheric transport and diffusion models for unmitigated releases which predict potential downwind concentration and dose to the workers and the public. Several similar models are available to perform the assessment, all based on Gaussian dispersion methodology. MELCOR Accident Consequence Code System Version 2 (MACCS2) (US DOE, 2004) and Generation II Environmental Radiation Dosimetry Software System (GENII) (Napier, 2011) are two of the radiological consequence codes that are available through the DOE Central Registry of safety software (DOE, 2013). The Gaussian dispersion methodology enables an analyst to take a large meteorological data set, spanning a large range of possible atmospheric dispersion conditions, and calculate cumulative frequency statistics of predicted time-averaged plume and potential consequences (Hanna et al., 1982). However, this methodology uses several simplified environmental characteristics (Miller and Hively, 1987) such as temporally- and spatially-uniform meteorological conditions, discrete plume diffusion modes based on typing atmospheric stability; applying roughness length and zero-plane displacement parameters to describe frictional drag imposed by the ground surface, and deposition velocity algorithms to describe an average rate of plume depletion by surface contact.

HTO has been shown to have a complex behavior with the environment. It behaves like water vapor in terms of its interactions with soil and vegetation, but is also subject to uptake and respiration processes. Lee et al. (2012) identified that for facility safety basis modeling, a 2 hour residence time of HTO within vegetation or soil should be used, which represents a fairly rapid cycling of HTO in and out of the environment relative to the 24 hour period typically used for dose assessment calculations. Its interactions with soil are further dependent on the soil moisture conditions (Garland 1979). Galeriu and Melintescu (2015) identify that more detailed understanding of the transfer of HTO between the atmosphere, soil and vegetation is still needed and is an important component for accurately performing dose modeling for accident analyses.

The UFOTRI model (Raskob 1999) has been the most widely used model specifically designed to assess the movement of tritium in the environment. A sensitivity analysis identified that interactions with the surface and vegetation contain the most (Galeriu et al. 1995). A potential shortcoming with UFOTRI and

similar models is that, once deposition has occurred, the deposited material remains in that location unless the model accounts for potential resuspension of deposited material. In complex environments, it is possible that movement of the deposited material could occur on rapid timescales. For instance, within a forest canopy, there can be transport within the airspace of the canopy that is distinctly different from the surrounding environment above the canopy. A closer examination of the complex environment may yield interesting facets of transport that would not be captured by the traditional Gaussian models.

Gaussian models typically assess deposition using a single deposition velocity which is designed to account for the complex interactions at the surface using a single number to describe the net effects. This parameter is based on a range of measurements and is highly site- and environment-specific. For this reason, we have undertaken a detailed study of the forested environment at the Savannah River Site (SRS) to assess the range of deposition velocities in the forest and identify what would be considered a conservative deposition velocity for use in safety basis modeling.

A forested environment has a spatially-variant wind flow and turbulence regime; separate and distinct from the free atmosphere above it. Several earlier analyses of wind structure in forested environments have shown that wind direction changes within the forest canopy (Smith et al., 1972), and that the standard logarithmic wind profile is not maintained due to frictional effects of the forest (Garratt, 1980; Parlange and Brutsaert, 1989). While the zero-plane displacement parameter partially accounts for this change by shifting the logarithmic wind profile upward to a more representative height, it does not account for deposition, which is permanently removing material onto an idealized surface. Accordingly, the Gaussian model is much too constrained to accurately depict ongoing HTO transport and fate as it moves from the free atmosphere to the forest canopy atmosphere and then to the understory atmosphere, before recycling back to the free atmosphere.

The presence of a separate flow regime below the forest canopy transports HTO horizontally at a different rate within the forest compared to its transport rate above the forest. Ejection and sweep events (i.e., strong bursts of upward and downward vertical motion across the forest boundary) result in intense turbulent motions (Zhu et al., 2007, Guo et al., 2010), propelling HTO into the forest, or flushing it out of the forest and back into the free atmosphere at a rapid rate (Rannik et al., 2016). While the effects may be minimal through the depth of the plume, the effects on near-surface concentration has a direct impact on the determination of radiological consequences.

In addition, forest vegetation absorbs HTO from the atmosphere as part of natural photosynthetic and evapotranspiration processes (Canadian Nuclear Safety Commission, 2009). The removal of HTO from the atmosphere through the mixing and absorption processes can be inferred in the standard Gaussian models from a determination of a deposition velocity. However, most of the HTO that is taken up by vegetation in the canopy region is returned to the atmosphere through resuspension, with a half-life of less than one hour (Brudenell et al., 1997; Boyer et al., 2009), leading to the conservative assumption of no deposition. Moreover, these processes will lead to some HTO redistribution well into the forest understory where it will be affected by additional mechanical shear and by changes in both wind direction and wind speed. Unfortunately, the extent to which the forest environment acts to further

disperse an airborne plume and how this enhanced dispersion affects net deposition velocity and plume centerline has not yet been fully researched. While these processes are far too complex to capture in a Gaussian modeling architecture, it may be possible, with a more comprehensive model, to determine a representative deposition velocity for HTO that captures a physically realistic net effect on the plume.

With this objective in mind, the Savannah River National Laboratory (SRNL) performed a review of dispersion modeling methodology for HTO, mainly in response to findings issued by the Defense Nuclear Facility Safety Board (DNFSB, 2011). The DNFSB was concerned that the application of a specified deposition velocity (i.e., 0.5 cm s^{-1}) in design safety analysis modeling of HTO plumes at SRS was not supported by current scientific understanding and may not be sufficiently conservative to ensure that no adverse worker or public health risk existed in the event of a release of HTO. A subsequent study by Murphy et al. (2012) examined experimental data collected at SRS on the uptake processes and subsequent resuspension of HTO from surface vegetation. This study concluded that the time scale of uptake and resuspension was of sufficiently short duration that no net deposition would occur during the integration period (i.e., approximately 24 hours) considered by safety-related radiological consequence assessments. As a result, the report recommended that modeling for design safety analysis should not credit removal of HTO by deposition in order to maintain a sufficiently conservative upper-bound for dose estimates at key downwind receptors. It should be emphasized that the DNFSB studies used the aforementioned, limited Gaussian modeling techniques, which made it impossible for it to examine the potential influence of the forest on fate and transport (Viner, 2012). Since the presence of extensive forests at SRS creates a micrometeorological environment where wind speed and wind direction will vary from above to below the forest canopy, the application of a Gaussian plume model is not sufficiently robust to capture these complex dispersion patterns. The current study seeks to quantify a deposition velocity that serves as a surrogate for the effective removal of HTO, with respect to a downwind receptor of concern, due to enhanced dispersion resulting from the complex interactions of the plume within the forest canopy and understory.

To demonstrate a more realistic value of deposition velocity, measurements from the Aiken AmeriFlux tower at the SRS were used as input to an atmospheric transport model, which can address two separate flow regimes above and within the forest. This coupled model was developed to quantify the movement of an airborne effluent from the free atmosphere as it moves in and out of the confined forest canopy and understory atmospheres. The SRNL model enables an estimation of the potential decrease in near-surface concentrations that result in comparison to using a simple Gaussian model. Accordingly, the magnitude of the predicted flux can be used to determine suitable deposition velocity magnitudes for use in simpler Gaussian models. In addition to improving the understanding of how forests influence dispersion, this model can also inform decisions regarding the determination of appropriate values of deposition velocity in highly complex environments.

2. Methodology

2.1 Description of the Coupled Dispersion Models

The coupled dispersion model developed for this study consists of: (1) A Gaussian model to simulate atmospheric dispersion above the tree canopy (z >/= 25 m); and, (2) An advection-diffusion model of transport to simulate transport within the forest (z < 25 m), where z is the height above the ground. The traditional Gaussian model concentration in three dimensions for an elevated release is represented by Equation 1:

$$C(x,y,z) = \frac{Q}{2\pi U \sigma_y \sigma_z}\left(e^{\frac{-y^2}{2\sigma_y}}\right)\left[\left(e^{\frac{-(z-h)^2}{2\sigma_z}}\right)+\left(e^{\frac{-(z+h)^2}{2\sigma_z}}\right)\right] \quad (1)$$

where, *C* is the concentration at any (x, y, z) point downwind, *Q* is the source term, *U* is the wind speed, σ_y and σ_z are diffusion parameters for the horizontal and vertical planes, respectively, and h is the source height. The plume was initialized as a point release of thirty-minute duration at a height of 61-m. The release height was chosen because that is the approximate height of the tritium facility stacks at SRS. The selection of a surface height (i.e., zero-plane) for the Gaussian model is not necessarily clear since there is a gradual transition occurring between the turbulence characteristics above the canopy which is generated by mechanical turbulence (i.e., wind shear) and thermal turbulence (i.e., buoyancy) terms and the turbulence generated by the forest canopy which is more by mechanical means (Arya, 2001). The surface for the Gaussian model was selected to be at 25 m, which is the forest-free surface layer height, equivalent to the approximate height of the loblolly pine forest. Direct measurements at and below the forest height from the Aiken AmeriFlux tower were used to describe the more complex vertical wind profile through the forest and understory.

Values for σ_y and σ_z are determined from the standard deviations of the horizontal and vertical components of wind direction, respectively (Garrett and Murphy 1982). The value of σ_y is calculated with Equation 2:

$$\sigma_y = \sigma_a x\left[\frac{x^{-0.2}}{1.67+0.3\left(\frac{|1-x^{-0.2}|}{0.48}\right)^{0.5}}\right] \quad (2)$$

where x is the downwind distance the plume has traveled and σ_a is the standard deviation of the horizontal wind direction. The determination of σ_z is based on the Pasquill stability class, calculated as a function of σ_e based on EPA protocols (EPA 2000, Hunter 2012) and downwind distance from the source, as shown in Equations 3a-3f:

A Stability	$\sigma_z = 0.20x$	(3a)
B Stability	$\sigma_z = 0.12x$	(3b)
C Stability	$\sigma_z = 0.08x(1+2*10^{-4}x)^{-0.5}$	(3c)
D Stability	$\sigma_z = 0.06x(1+1.5*10^{-4}x)^{-0.5}$	(3d)
E Stability	$\sigma_z = 0.03x(1+3*10^{-4}x)^{-1}$	(3e)
F Stability	$\sigma_z = 0.02x(1+3*10^{-4}x)^{-1}$	(3f)

Most models use a deposition velocity to predict the effect of plume material settling on the surface. Here, we are interested in assessing what the deposition velocity should be, so we instead attempt to explicitly model the deposition processes as movement of HTO into the forest, transfer between

different levels of the forest, and movement from the air into the vegetation and the soil. Deposition velocity is then calculated for each scenario and a distribution of calculated deposition velocities will be used to determine the 1st and 5th percentile deposition velocity which would correspond to the more conservative rates of deposition which we would look to apply in safety basis modeling. The mass of HTO predicted to move into the forest from the free atmosphere above it is then used as a source term for the advection-diffusion transport model that predicts transport within the forest. In a similar manner, resuspension in this model refers to the upward flux of airborne material from the forest canopy back to the free atmosphere. Where the canopy portion of the plume was predicted to exceed the concentration of the free atmosphere above it, the flux calculation yielded a negative deposition velocity which was treated as a resuspension velocity separate from the deposition velocity.

The downwind effects of HTO deposition (i.e., downward flux of HTO from the free atmosphere to the forest canopy atmosphere) on the Gaussian plume was modeled by applying negatively-sourced Gaussian plumes originating at the points of deposition. In a similar manner, the resuspension of HTO (i.e., upward flux from the forest canopy atmosphere to the free atmosphere) was modeled as positively-sourced Gaussian plumes. This technique created a family of overlapping plumes which, when summed with the original plume, predicts the resulting downwind concentration including full HTO recycling through the forest environment.

Transport within the forest was modeled by first dividing the forest into a 10-meter downwind grid (dx = 10 m) with four vertical levels, which spanned lower and upper understory levels (i.e., 0-7 m, 7-15 m) and lower and upper canopy levels (i.e., 15-20 m, 20-25 m), centered around the four measurement heights of the Aiken Ameriflux Tower located within or below the forest canopy. This is shown in Figure 1. Transport within the forest canopy and understory was modeled using an advection diffusion method (Egan and Mahoney 1972), as shown in Equation 4:

$$\frac{\partial \mathrm{C}}{\partial \mathrm{t}} = -\mathrm{u}\frac{\partial \mathrm{C}}{\partial \mathrm{x}} - \mathrm{v}\frac{\partial \mathrm{C}}{\partial \mathrm{y}} - \frac{\partial}{\partial \mathrm{z}}\mathrm{K}\frac{\partial \mathrm{C}}{\partial \mathrm{z}} \quad (4)$$

where C is concentration, u and v are the horizontal wind speeds in the x- and y- directions, respectively, and K is the vertical turbulent diffusivity. The term on the left represents the change in concentration with time. The first term on the right-hand side of the equation is the downwind transport of the concentration at each height level within the grid. The third term describes the diffusion between vertical levels as a function of the vertical concentration gradient between adjacent levels and the atmospheric resistance between these levels and is treated in a manner identical to that of the Gaussian model (Garrett and Murphy, 1982). The horizontal diffusion and vertical advection terms, which are not shown in Equation 4, have been omitted since they are negligible compared to the horizontal advection and vertical diffusion terms. At each of the 4 levels, the meteorological conditions were modeled using half-hourly averaged meteorological data from a 20-Hz sonic anemometer located at each measurement level of the tower; allowing the model to account for changing wind direction with height above ground. This wind direction change introduces a mechanical shearing effect on the plume since it could travel in different directions based on the variable wind conditions at each level.

Flux of HTO into the vegetation is driven by the concentration gradient between the atmosphere and the vegetation. Many models simulate the rate of uptake or respiration by the vegetation by calculating resistance terms to describe how easy or difficult it is for HTO to move between the atmosphere and the vegetation (Uptake source). We use the method described by Garratt and Murphy (1982) which is based on measurements of HTO releases and accounts for differences between daytime and nighttime scenarios due to stomatal opening and closing. HTO moves into this vegetation when the HTO concentration is lower within the vegetation than the atmosphere, and HTO moves back to the atmosphere when the concentration was greater within the vegetation than the atmosphere. Soil flux of HTO was also simulated for the lower understory levels following the same modeling approach used for vegetation that describes the rate of transfer as a function of the concentration gradient between the lowest level of the model and the soil..

Plume depletion was quantified at the 25-m level by comparing the baseline Gaussian model in which it was assumed that no deposition occurred (i.e., deposition velocity = 0.0 cm s^{-1}) to the new coupled modeling framework that addresses the effects of forest interactions on the HTO plume. Of great interest were the concentrations 10 km from the HTO release at the edge of the SRS site boundary, where offsite populations could be affected.

2.2 Meteorological Measurements

The Aiken AmeriFlux tower is a 30-m high walk-up tower equipped to measure micrometeorological variables at the 2-m, 12-m, 18-m, 25-m and 28-m levels. It had continuously monitored key meteorological variables during its 39-month operation between February 2011 and April 2014. Each level of the tower is instrumented with a 20-Hz sonic anemometer (i.e., CSAT3; Campbell Scientific, Logan, Utah, USA) to measure three-dimensional winds (u, v, w) and virtual temperature (T_v) along with an open-path CO_2/H_2O gas analyzer (i.e., LI-7500; Li-Cor Biosciences, Lincoln, NE, USA) to measure ambient CO_2 and water vapor concentrations. The instruments monitored the meteorological conditions by taking samples at 20 Hz which were then binned into 30-minute averaging periods. Averages of wind speed, wind direction and water vapor, as well as water vapor flux, were calculated for each 30-minute period. Periods which had missing values for greater than 10% of the period at any of the five levels were considered incomplete and subsequently removed.

A total of 12,615 periods were identified where 30-minute averages of the data required for this analysis were available at all five levels of the AmeriFlux tower. Cases were then further down-selected to ensure that no rain had occurred in the previous 6 hours (i.e., instruments were dry), and that the wind was blowing in a sector from 90 degrees clockwise to 270 degrees (i.e., East-West). Since the tower instruments are mounted on booms extending 5 m to the south of the tower, this latter condition was imposed to ensure that mechanical turbulence from the tower structure, which would obfuscate the data, was minimized. Another reason for selecting this downwind sector was to ensure a relatively homogenous fetch over the forest landscape so that the measured flow could not be not influenced by local agricultural or industrial regions which have significantly different roughness lengths. After accounting for these constraints, 5,963 periods remained for analysis.

To account for potential biases related to the tilt of the sonic anemometers, as well as from gently sloping topography, a planar fit was applied to the measurement data prior to analysis. The planar fit was performed following a technique which imposes a coordinate transformation to ensure that the mean vertical velocity is zero (Wilczak et al., 2001). Additional corrections to account for density fluctuations were applied following a barometric pressure-related methodology (Webb et al., 1980). The pressure measurements required for performing the density fluctuation corrections were taken from 15-minute averages from a sensor located near the center of the SRS, approximately 10 km from the Aiken AmeriFlux tower. With respect to this technique, the pressure data were judged to be spatially representative.

The atmospheric stability category used for determining the σ_z was based on the standard deviation of the vertical wind direction, σ_e, measured at the Climatology Tower at SRS, a 61-m tower located 17-km away at the center of SRS. The range of σ_e recommended by the EPA (2000) for each Pasquill stability class is representative of flat environment with a roughness length of 15 cm and wind measurements taken at 10 m. EPA-recommended corrections were applied to account for differences in roughness length (160 cm), displacement height (18 m), and the height of wind measurements (61 m) of the forest at SRS (US EPA, 2000, Weber et al., 2012).

3. Results

3.1 Summary of Meteorological Measurements and Turbulence Typing

To ensure that the range of meteorological conditions were temporally representative of the overall climatological conditions of the region, a comparison of stability classes was conducted between the simulated periods and a five-year climatology of stability class at SRS, as shown in Figure 2. Individual periods were binned according to the six Pasquill stability classes, where Class A is the most unstable, Class D is a neutral stability, and Class F is the most stable. There are only small differences in the stability class distribution and this pattern is reasonably representative of the general climatological conditions in the region.

Figure 3 presents the results of an analysis to determine the magnitude of wind direction changes with height in the forest canopy and understory. The counter-clockwise (CCW) and clockwise (CW) changes in 20-degree azimuth increments of the wind direction at each level was determined relative to the 28-m level of the AmeriFlux tower, which is representative of the prevailing wind direction above the forest canopy. This analysis showed that wind shear occurred at all levels of the forest, and the shear was greater in magnitude in the understory regions of the forest canopy, which was the expected outcome. At the top of the forest canopy, represented by the 25-m level, the data show that very little shearing occurred (i.e., more than 95% of the cases exhibited wind direction changes of less than 20° azimuth). Deeper into the lower canopy, represented by the 18-m level, 70% of cases exhibited wind direction changes less than 20° azimuth, as the canopy effects on the wind field became more pronounced. At the lower and upper understory levels (i.e., 2-m and 12-m levels, respectively), the cases which exhibited wind direction changes less than 20° azimuth, dropped to 40% and 46%, respectively, suggesting that within the understory, the wind direction is often greater than 20° azimuth different

than above the canopy. The distribution of winds turning to the right (i.e., CW) or to the left (i.e., CCW), moving downward through the forest canopy was nearly even.

3.2 Summary of Dispersion, Deposition and Resuspension Characteristics

Figures 4 through 6 present a summary of the deposition velocity, resuspension velocity, and net deposition velocity, respectively, that was calculated by the coupled model. The deposition velocity in Figure 4 represents the transfer of HTO from the free atmosphere above the forest to the canopy atmosphere. Deposition velocities ranged from 0.6 cm s^{-1} to 17.9 cm s^{-1}, with the highest values occurring during unstable and neutral stability classes and a slightly lower upper bound during stable stability cases. The highest mean values of deposition velocity occurred in weakly unstable and neutral cases (i.e., C and D stability), while minimum values of deposition velocity were about the same for all stability classes.

In Figure 5, the resuspension velocity, which represents the transfer of HTO from the canopy atmosphere back into the free atmosphere, exhibited a similar pattern of mean and minimum values across all stability classes, with a slight increase in the mean occurring for neutral stability.

Summing the deposition velocity and resuspension velocity for each case produced a 'net deposition velocity', which ranged from 0.1 cm $s^{-1}$to 17.6 cm s^{-1}, as shown in Figure 6. The distribution of net deposition velocity by stability class was virtually the same as the calculated deposition velocity, which is again expected given that the range of deposition velocity was more than twice that of resuspension velocity, and more than four times greater in the unstable cases. For all stability classes, the magnitude of the mean deposition velocity was 2 to 3 times greater than the magnitude of the resuspension velocity.

4. Discussion

Murphy, et al. (2012) had earlier concluded conservatively that in the context of modeling an HTO release for safety-related radiological consequence assessments, no deposition should be considered in radioactive consequence calculations. This conclusion was based on the premise that the cycle of deposition, uptake, and resuspension of HTO in the environment occurs on very short time scales, ranging from minutes to hours. While this behavior is generally true, radiological consequence models are typically Gaussian which are unable to address the physics of a plume interacting with the surface environment in any way except through simple dry deposition processes. While the conventional approach of using Gaussian models without credit for deposition provides an upper bound for plume concentrations and radiological consequences, additional comprehensive parameterization of the HTO recycling process could provide analysts a means to calculate more realistic values. SRNL has examined how complex forested environments may be characterized by modeling the dispersion of an HTO plume over a forested region using a more comprehensive modeling scheme that has been calibrated by a statistically-significant sample of wind measurements spanning the forest environment from the forest floor to a few meters above the forest canopy.

Figure 7 presents an example of the modeled concentrations at each level of the model. The figure illustrates how HTO can move from the free atmosphere at the 28-m level into the lower-level canopy and understory areas. During the plume passage, the HTO concentrations in the forest canopy atmosphere are roughly an order of magnitude less than the free atmosphere. Following the plume passage, the model levels within the forest quickly come to a near-equlibrium at all levels. Resuspension from the forest is also observed to occur, with the 28-m level remaining approximately an order of magnitude below the within-canopy concentration. The HTO concentration within the canopy had a tendency to drop only slowly following the plume passage, indicating the potential for HTO to be held up within the forest airspace for a substantial amount of time after the initial plume passes.

The deposition velocities estimated in this study ranged from 0.6 cm s^{-1} to 17.9 cm s^{-1}. Compared to other published deposition velocities, such as between 0.1 and 10 cm s^{-1} (Galeriu et al., 2008), the model predicted range appears somewhat high. However, it should be noted that previously reported deposition velocities, as well as those applied in commonly-used radiological consequence dispersion models, are single values that encompass all stages of HTO transfer from the atmosphere into vegetation or the soil matrix. Earlier studies did not use a coupled advection model.

The predicted values represent not only direct plume deposition through vegetative absorption, but also the rate of transfer of HTO from the free atmosphere into the canopy atmosphere. Once in the understory layer, the SRNL coupled model transports HTO within the forest, often in a direction different from the prevailing free atmosphere wind direction, as shown in Figure 3. This wind shear shows that the model is advecting the peak canopy and understory atmospheric concentrations away from the centerline of the free atmosphere plume, which in turn, allows greater sustained downward flux of HTO compared to that of a simple Gaussian model that is unable to account for the micrometeorological conditions within the forest. This further lowers the peak centerline concentrations of the airborne plume and produces and increase in deposition velocity.

Typical deposition velocities only describe the rate of HTO movement from the free atmosphere above the canopy to within the canopy. Since this study is not focused on deposition to surfaces but to a distinctly separate atmosphere, how HTO moves from within the forest canopy back into the free atmosphere needs to be better understood. The modeling results revealed a range of predicted resuspension velocities that had similar extremes to the range of deposition velocities. However, the resuspension velocity was determined to be approximately one-third of the deposition velocity across all cases. A plausible reason for this behavior may be that the forest understory approaches equilibrium following the passage of the plume, thus limiting the upward flux from the understory. This equilibrium may result from HTO deposition to the soil matrix occurring over longer time frames than the downward flux of HTO from the canopy levels of the forest to the understory level. In the example shown in Figure 7, the concentration gradient between the 2-m and 12-m understory levels would continue to drive HTO downward well after the plume passes, but as the magnitude of the gradient approaches zero, the downward transfer rate slows. If deposition to the soil matrix is a slower process than the downward flux of HTO, peak levels will exist somewhere else in the canopy or upper understory layer of the forest rather than near the surface for an elevated release occurring above the canopy.

The influence of the forest, in terms of percent plume depletion, was remarkably similar at the two distances, indicating that forest size may not play an appreciable role beyond a certain distance, and that any change in the magnitude of HTO concentration that enters the forest canopy and understory air is primarily dependent on the ambient air concentration. Figure 8 (top) shows the percent of plume depletion at 1 km, while Figure 8 (bottom) shows depletion at 10 km from the above-forest atmosphere relative to a Gaussian model that does not include transport and interactions within a forest environment. Slightly greater percentages of depletion were noted after 10 km of travel, but the average depletion was increased by less than 3% for unstable and neutral cases and increased by less than 5% for stable cases. This conclusion would suggest that the size of the forest does not affect the rate of plume depletion, but that larger forests will result in greater plume depletion.

To develop a net deposition velocity that could be used in radiological consequence models, the resuspension velocity was subtracted from the deposition velocity. In all cases there was a net loss of material (i.e., depletion), since the deposition velocity was always greater than the resuspension velocity. With respect to design safety basis calculations, the lowest values of net deposition are typically of greatest interest as this limits the amount of plume loss and ensures conservatism in atmospheric plume concentrations. In this study, the 5^{th} and 1^{s} percentile of net deposition velocities, which would lead to more conservative results, are 1.2 cm s^{-1} and 0.7 cm s^{-1}, respectively, which is more closely aligned with the range of reported deposition velocities.

5. Conclusions

This study also clearly demonstrates that a significant reduction in HTO concentration at the centerline of the airborne Gaussian plume occurs through migration of HTO deep into the forest canopy and understory atmosphere, and where the material can be transported in a direction that is different than the above-canopy winds. In this way, while the HTO that is deposited into the forest may return to the atmosphere over a relatively short time scale, its return to the free atmosphere may occur some distance away from the original plume centerline.

In all the study cases, some finite net deposition occurred, and the airborne concentrations predicted by the coupled model were around 60% lower at a receptor distance of 10 km than the results from the conventional Gaussian atmospheric transport models currently used in design accident analysis. Since the predicted radioactive dose varies linearly with air concentration, it is estimated that the worst-case potential dose determined from current models may be overpredicted by a factor of 1.5. The results presented in this paper suggest that there is a reasonable and defendable basis for using a non-zero deposition velocity in these models, which still maintains conservatism, while acknowledging the mitigating effects of the forest on plume concentration and calculated dose at a downwind receptor.

Acknowledgements

This work was funded by SRNL Laboratory-Directed Research and Development Program (LDRD-2015-00068), Savannah River Tritium Facility's Project Directed Research and Development Program (Project SR19031), and the National Nuclear Security Administration Nuclear Safety Research and Development Program.

References

Arya, S.P., 2001. Introduction to Meteorology. Academic Press, 420 pp.

Boyer, C., Vichot, L., Fromm, M., Losset, Y., Tatin-Froux, F., Guetat, P., Badot, P.M., 2009. Tritium in plants: A review of current knowledge. Env. And Exp. Bot. 67, 34-51.

Brudenell, A.J.P., Collins, C.D., Shaw, G., 1997. Dynamics of tritiated water (HTO) uptake and loss by crops after short-term atmospheric release. J. of Env. Rad. 36, 197-218.

Canadian Nuclear Safety Commission, 2009. Investigation of the environmental fate of tritium in the atmosphere. INFO-0792. 110 pp.

Defense Nuclear Facility Safety Board, 2011. Review of Safety Basis, Tritium Facilities, Savannah River Site. DNFSB Staff Issue Report, Washington, DC.

Egan, B.A., Mahoney, J.R., 1972. Numerical modeling of advection and diffusion of urban area source pollutants. J. Appl. Met. 11, 312-322.

Environmental Protection Agency, 1988. Limiting values of radionuclide intake and air concentration and dose conversion factors for inhalation, submersion, and ingestion. Federal Guidance Report No. 11, EPA-520/1-88-020, 234 pp.

Environmental Protection Agency, 2000. Meteorological monitoring guidance for regulatory modeling applications. EPA-454/R-99-005, 171 pp.

Galeriu, D., Davis, P. A., Chouhan, S., Raskob, W., 1995. Uncertainty and sensitivity analysis for the environmental tritium code UFOTRI. Fusion Science and Technology, 28, 853-858.

Galeriu, D., Davis, P., Raskob, W., Melintescu, A., 2008. Recent progresses in tritium radioecology and dosimetry. Fusion Sci. and Tech. 54, 237-242.

Galeriu, D., Melintescu, A., 2015. Progresses in tritium accident modeling in the framework of IAEA EMRAS II. Fusion Science and Technology, 67, 343-348.

Garland, J. A., 1979. Transfer of tritiated water vapor to and from land surfaces. International Atomic Energy Association. Nuclear Energy Agency, Proceedings Series, Paris, France. 349-358.

Garratt, J.R., 1980. Surface influence upon vertical profiles in the atmospheric near-surface layer. Q. J. of the Royal Meteorol. Soc. 105, 1079-1082.

Garrett, A.J., Murphy, C.E., 1982. A puff-plume atmospheric deposition model for use at SRP in emergency response situations. DP-1595. 76 pp.

Guo, H., Boroduilin, V.I., Kachanov, Y.S., Pan, C., Wang, J.J., Lian, Q.X., Wang, S.F., 2010. Nature of sweep and ejection events in transitional and turbulent boundary layers. J. Turbulence. 11, DOI: 10.1080/14685248.2010.498425

443 Hanna, S.R., Briggs, G.A., Hosker, R.P., 1982. Handbook on atmospheric diffusion. DOE/TIC-11223. 110
444 pp.

445 Hunter, C.H., 2012. A recommended Pasquill stability classification method for safety basis atmospheric
446 dispersion modeling at SRS. SRNL-STI-2012-00055, Revision 1. 26 pp.

447 Lee, P., Murphy, C., Viner, B., Hunter, C., Jannik, T., 2012. Recommended tritium oxide deposition
448 velocity for use in Savannah River Site safety analyses. SRNL-STI-2012-00128.
449 https://www.osti.gov/servlets/purl/1038895/

450 Kessler, G., 1983. Nuclear Fission Reactors. Springer-Verlag Wien, 258 pp.

451 Miller, C.W., Hively, L.M., 1987. A review of validation studies for the Gaussian plume atmospheric
452 dispersion model. Nucl. Safety. 4, 522-531.

453 Murphy, C.E., Lee, P.L., Viner, B.J., and Hunter, C.H., 2012. Recommended tritium oxide deposition
454 velocity for use in Savannah River Site safety analyses. SRNL-STI-2012-00128, Revision 1. 36 pp.

455 Napier, B.A., 2011. GENII Version 2 Users' Guide. PNNL-14583 Rev. 3, Pacific Northwest National
456 Laboratory, Richland, Washington.

457 Ojovan, M.I., Lee, W.E., 2005. An Introduction to Nuclear Waste Immobilization. Kidlington, Oxford.

458 Parlange, M., Brutsaert, W., 1989. Regional roughness of the Landes forest and surface shear stress
459 under neutral conditions. Bound. Layer Meteorol. 48, 69-81.

460 Rannik, U., Zhou, L., Zhou, P., Gierens, R., Mammarella, I., Sogachev, A., Boy, M., 2016. Aerosol dynamics
461 within and above forest in relation to turbulent transport and dry deposition. Atmos. Chem. and Phys.
462 16, 3145-3160.

463 Raskob, W., 1999. The present status and recent applications of the accidental tritium assessment code
464 UFOTRI. JAERI-Conf-99-001. Amano, Hikaru (Ed.).
465 https://inis.iaea.org/collection/NCLCollectionStore/_Public/30/031/30031661.pdf

466 Smith, F.B., Carson, D.J., Oliver, H.R., 1972. Mean wind-direction shear through a forest canopy. Bound.
467 Layer Meteorol. 3, 178-190.

468 US Department of Energy, 2003.

469 US Department of Energy, 2004. MACCS2 computer code application guidance for documented safety
470 analysis. DOE-EH-4.2.1.4-MACCS2. 253 pp.

471 US Environmental Protection Agency, 2000. Meteorological monitoring guidance for regulatory
472 modeling applications. EPA-454/R-99-005. 171 pp.

473 Viner, B.J., 2012. Modeling tritium transport, deposition, and re-emission. SRNL-STI-2012-00131. 21 pp.

474 Webb, E.K., Pearman, G.I., Leuning, R.G., 1980. Correction of flux measurements for density effects due
475 to heat and water-vapor transfer. Q. J. of the Royal Meteorol. Soc. 106, 85-100.

476 Weber, A.H., Kurzeja, R.J. and Hunter, C.H., 2012. Roughness lengths for the Savannah River Site. SRNL-
477 STI-2012-00016. 33 pp.

478 Wilczak, J.M., Oncley, S.P., Stage, S.A., 2001. Sonic anemometer tilt correction algorithms. Bound. Layer
479 Meteorol. 99, 127-150.

480 Zhu, W., van Hout, R., Katz, J., 2007. On the flow structure and turbulence during sweep and ejection
481 events in a wind-tunnel model canopy. Bound. Layer Meteorol. 124, 205-233.

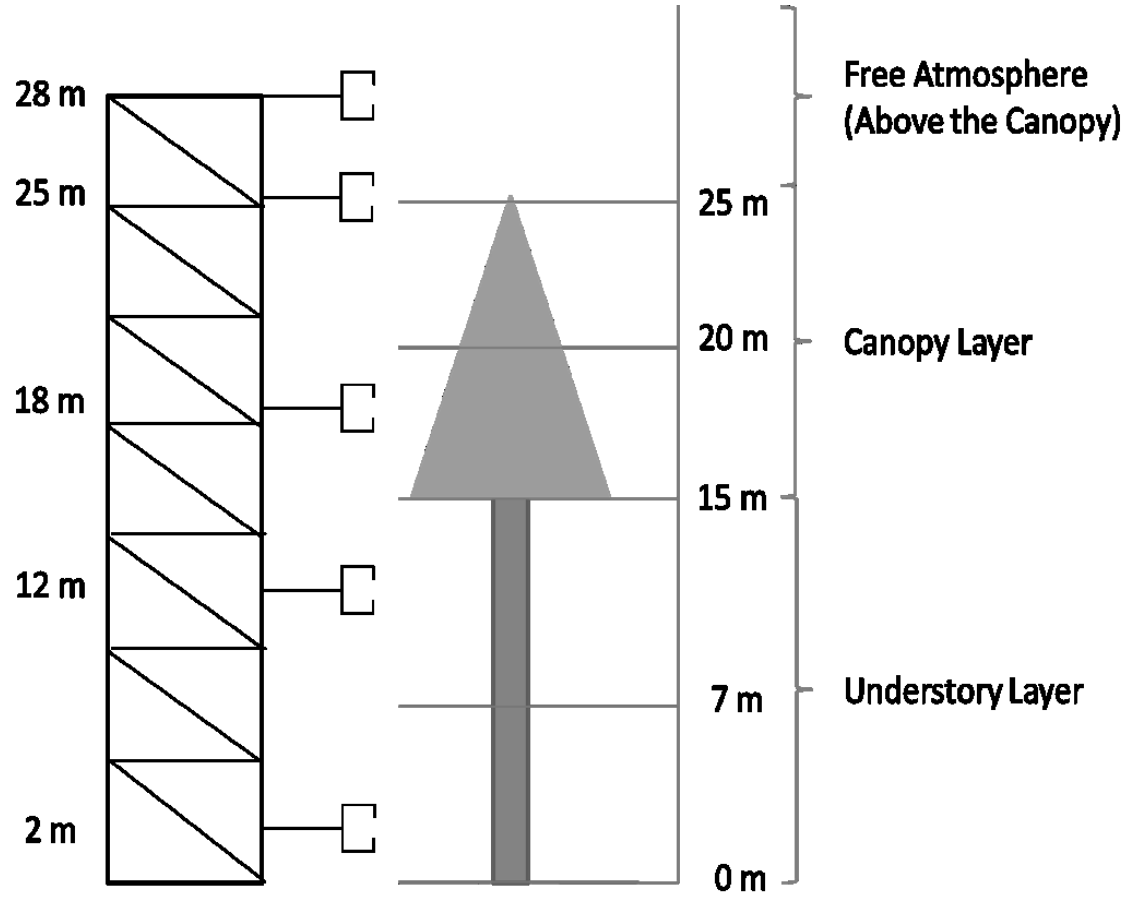

Figure 1: Illustration of the Aiken AmeriFlux tower and model levels relative to the pine forest canopy and understory.

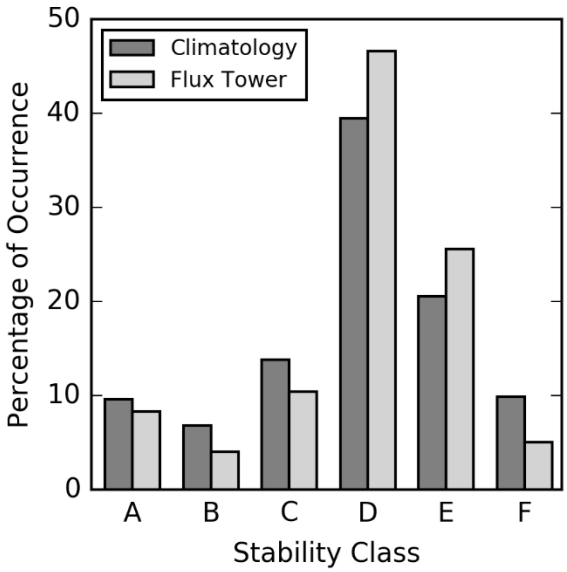

486

487 Figure 2: Comparison of stability classification frequencies at the Aiken AmeriFlux tower (black) and the
488 five-year climatological record taken at the Climatology tower at the Savannah River Site (gray).

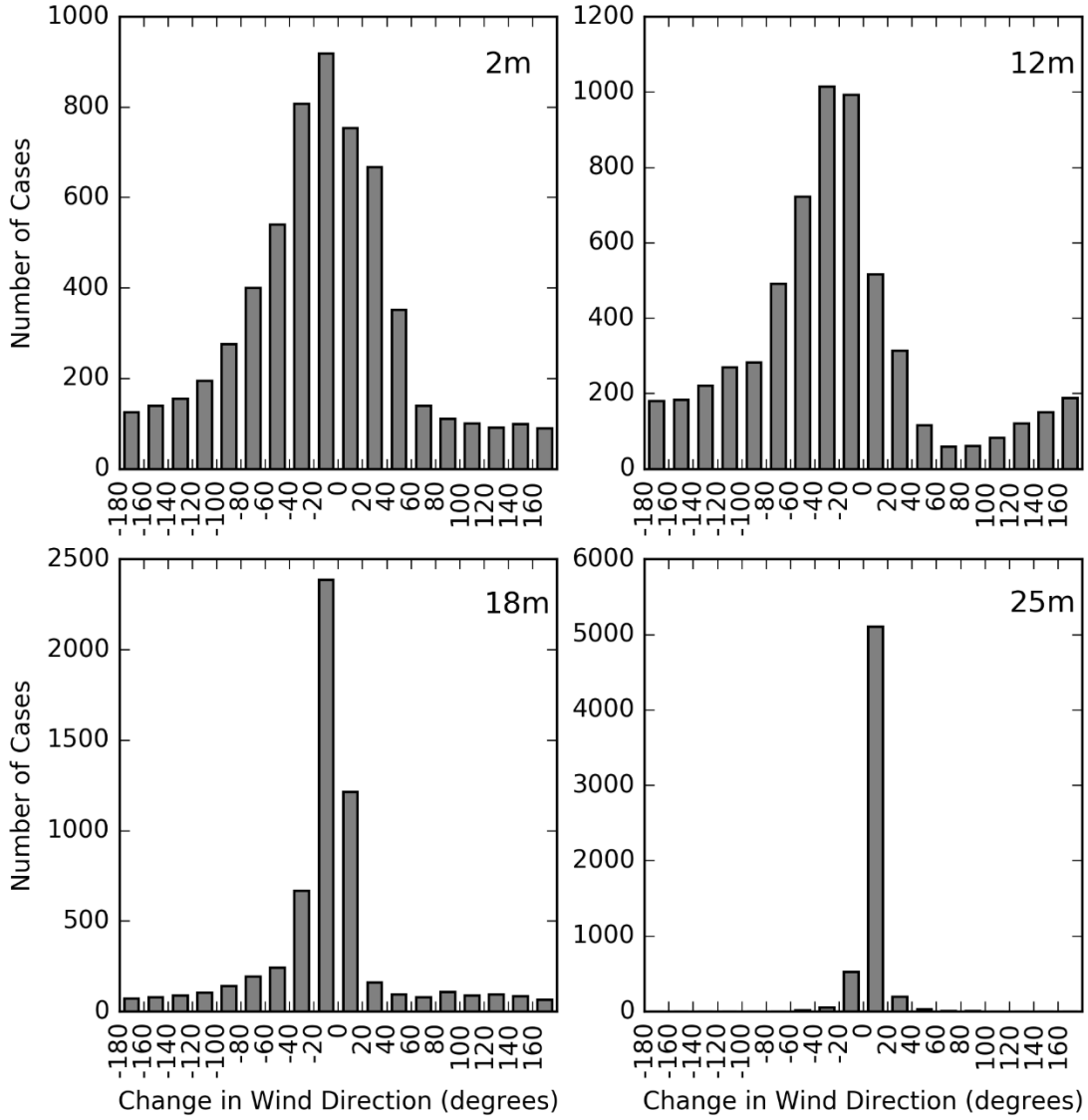

Figure 3: The change in wind direction between the 28m level and 2, 12, 18 and 25m levels. Negative changes in wind direction indicate a counter-clockwise shift while positive values indicate a clockwise shift from the 28m level. Bars indicate the number of cases which fell between the x-axis values (i.e., the number of cases between 0 and 20 degrees, between 20 and 40 degrees, etc.).

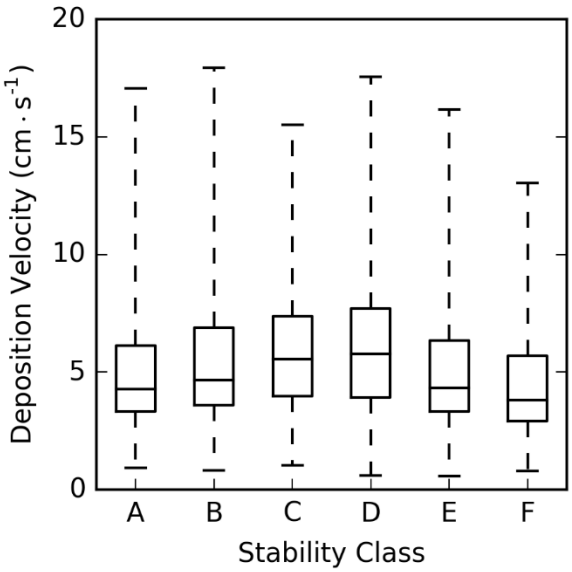

494

495 Figure 4: Range of modeled deposition velocity as a function of Pasquill stability class. The horizontal
496 lines in the boxes represent the 1st quartile, mean, and 3rd quartile values, while the whiskers represent
497 the full range of deposition velocity

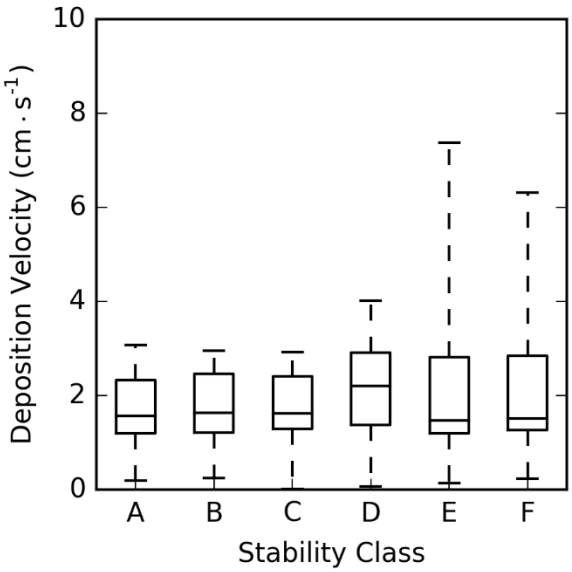

498

499 Figure 5: Range of modeled resuspension velocity as a function of Pasquill stability class. The horizontal
500 lines in the boxes represent the 1st quartile, mean, and 3rd quartile values, while the whiskers represent
501 the full range of resuspension velocity.

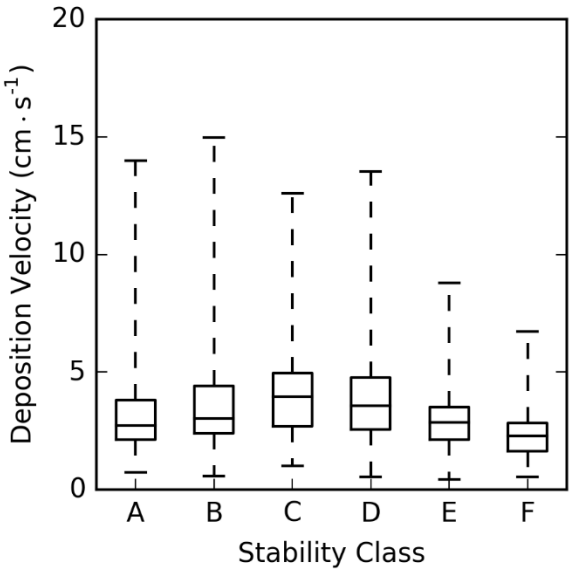

502

503 Figure 6: Range of modeled net deposition velocity as a function of Pasquill stability class. The horizontal
504 lines in the boxes represent the 1st quartile, mean, and 3rd quartile values, while the whiskers represent
505 the full range of net deposition velocity estimates.

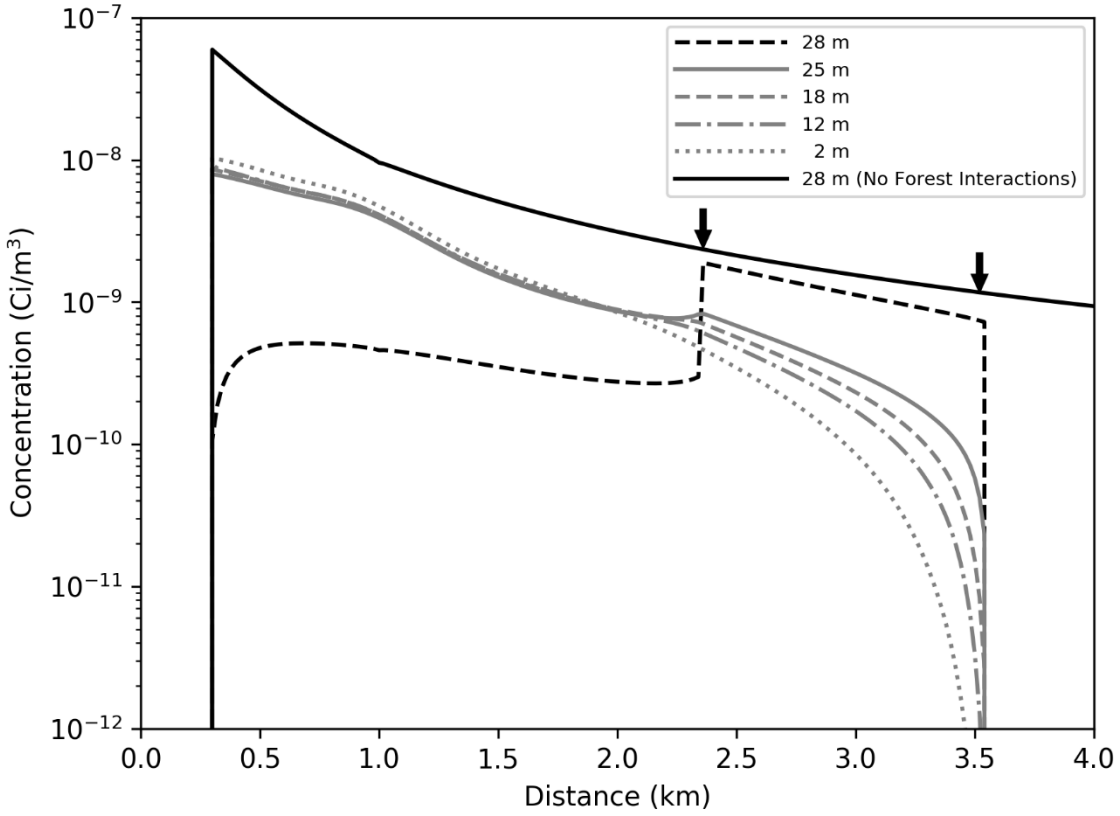

Figure 7: An example of the predicted HTO concentration. The solid black line indicates the expected concentration using a Gaussian model over the forest between 0.3 and 4.0 km, representing the baseline case. The dashed black line indicates the predicted concentration when forest interactions are included. Arrows indicate the leading (right) and trailing (left) edge of the plume resulting from a 30 minute release. Additional concentration to the left of the arrows represents resuspension from the forest at the 28m level. The gray lines indicate concentrations at model levels within the forest. The depiction represents a snapshot of dispersion 100 minutes following the release in an unstable (PG Stability Class 'A') atmosphere.

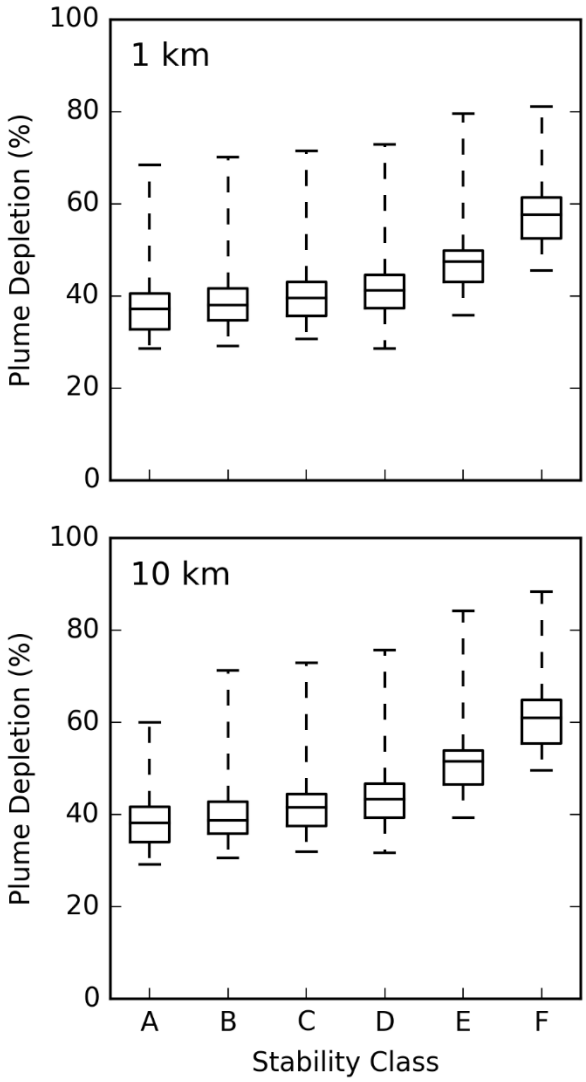

514

515 Figure 8: The percentage of plume depletion from the above-forest plume relative to a Gaussian model
516 that does not include transport and interactions within a forest environment for distances of 1 km and
517 10 km.